

The evolution of defects in a two-dimensional wet foam

B S Gardiner, B Z Dlugogorski[†] and G J Jameson

ARC Research Centre for Multiphase Processes, Department of Chemical Engineering,
The University of Newcastle, Callaghan, 2308, NSW, Australia

E-mail: cgbzd@alinga.newcastle.edu.au (B Z Dlugogorski)

Received 4 December 1998, in final form 5 May 1999

Abstract. This paper investigates the evolution of defects in two-dimensional (2D) wet foams by using the dynamic bubble simulation approach. Two defect types are considered: a single large bubble, and a cluster of small bubbles inserted in an otherwise monodisperse hexagonal lattice. In the case of a single large defect bubble, the disorder of the cluster associated with the defect is seen to increase and peak before returning to a state having a degree of order different from that of the disordered foam scaling state. This long-timescale behaviour agrees with recent 2D wet-foam experiments yet disagrees with the majority of existing simulations on dry foam. The inclusion of a finite liquid content in the present simulations is identified as a possible reason for the improved predictions. In the case of a defect of small bubbles, coarsening trends observed in experiments are reproduced. Unlike the case for a single large bubble defect, no peak was observed in the disorder of the bubble cluster.

1. Introduction

The evolution of a defect in an otherwise perfect 2D monodisperse bubble lattice has been receiving substantial attention in the recent literature. This is because the evolution of defects represents the initial stage of foam coarsening. In particular, the case of a single large bubble in an otherwise monodisperse hexagonal bubble lattice is currently being scrutinized due to the unexpected results from simulations performed by Levitan (1994). Using a mean-field approach, Levitan found that the second distribution moment of the number of neighbours per bubble, μ_2 , for bubbles within the cluster of bubbles disturbed by the defect seed bubble, reached a constant value. Levitan's result was in contrast to earlier expectations (Weaire 1995). On the basis of simulations (Weaire and Lei 1990, Herdtle 1991) and experiments (Aboav 1980, Stavans and Glazier 1989), which indicated that high values of μ_2 may be achieved, it was believed that μ_2 would grow indefinitely, or until the entire foam system reached a scaling state.

In the experiments of Stavans and Glazier (1989), μ_2 was seen to reach a maximum of ~ 2.6 for a nearly ordered hexagonal foam dispersed with large defects, before settling to a scaling state with $\mu_2 = 1.4 \pm 0.1$. When Stavans and Glazier started their experiments with a very disordered foam, a scaling regime was observed having the same μ_2 as the scaling regime of the initially ordered system. It was concluded that the scaling state occurred after all hexagonal regions, in the initially ordered foam, had been consumed by the defect sites. From the results of Stavans and Glazier (1989), who reported μ_2 for the entire system, it can

[†] Author to whom any correspondence should be addressed.

be inferred that the initial elevated value of μ_2 was due to the evolution of the scattered defects in the otherwise ordered lattice. Hence, recent simulations and experiments have concentrated on the evolution of a single defect, as do the present simulations.

Stavans and Glazier (1989) also reported variations of Plateau border angles away from 120° . The result of these angle variations was to discourage the appearance of bubbles with a large number of neighbours. This observation seems to contradict the conclusion often drawn from this study that μ_2 grows indefinitely. Instead it suggests that for real foams containing a finite liquid volume, μ_2 may not grow indefinitely, as there is an upper limit to the range of possible bubble sizes.

Another experimental result which has been used to infer an open-ended growth of μ_2 is that of Aboav (1980). Aboav did not see a scaling state, with μ_2 constantly increasing, eventually reaching 2.86 at the end of the experimental data set. Stavans and Glazier (1989) suggest that Aboav's failure to observe a scaling state was due to limitations in experiment duration.

Following Levitan's simulation results (Levitan 1994), a number of authors have made efforts to determine the origin of the discrepancy between Levitan's results and the expectations of other researchers. In the direct simulations of Ruskin and Feng (1995), Jiang *et al* (1995), and Chae and Tabor (1997), μ_2 was seen to grow for the bubble cluster and for the entire bubble foam system, and the number of neighbours of the initial defect bubble grows indefinitely (see figure 1(a)). That is, no scaling state such as that proposed by Levitan was observed. However, Jiang *et al* (1995) found that when the original large bubble was excluded from the evaluation of μ_2 for the bubble cluster, a special scaling state emerged with $\langle n \rangle = 5.5$ and $\mu_2 = 0.71 \pm 0.17$. In agreement with the direct simulations of Ruskin and Feng (1995) and Jiang *et al* (1995), Vaz and Fortes (1997) observed, in their 2D bubble raft experiments, no scaling state for either the bubble cluster or the entire foam system. They did however confirm the result of Jiang *et al* (1995), that a special scaling state exists for the bubble cluster with the original defect bubble excluded. In particular, Vaz and Fortes (1997) found that for the bubbles in the special scaling state, $\langle n \rangle = 5.2\text{--}5.6$ and $\mu_2 = 0.5\text{--}1.5$.

In recent experiments, Vaz and Fortes (1997), as well as Abd el Kader and Earnshaw (1997, 1998), used 2D bubble rafts to study a number of defect types, including a single seed bubble defect; see figure 1(b). Their experiments were limited in duration due to film breakdown and impingement of other defects on the defect studied. Therefore, these authors were unable to study experimentally the evolution of bubble defects at the longer times typical of simulations.

Another difference between the experiments of Vaz and Fortes (1997) and Abd el Kader and Earnshaw (1997, 1998) and previous simulations of the evolution of bubble defects is that, in experiments, the foam has a finite liquid content. Hence in experimental wet foams, vertex angles are not limited to 120° , an assumption that most previous simulations on defect evolution have made. Vertex angles of 120° imply dry foams. The present simulations however incorporate a finite liquid content allowing direct comparisons to be made with the experiments of Vaz and Fortes (1997) and Abd el Kader and Earnshaw (1997).

Most recently, Abd el Kader and Earnshaw (1998) reported on their bubble raft experiments carried out for longer timescales than earlier experiments (Vaz and Fortes 1997, Abd el Kader and Earnshaw 1997). Abd el Kader and Earnshaw (1998) found evidence to suggest that μ_2 does not grow indefinitely as was expected from earlier experiments and simulations. These authors also reported that both the number of neighbours of the defect bubble and μ_2 for the bubble cluster do not increase indefinitely but fluctuate about constant values at long timescales, in direct contradiction to simulations of defect growth in 2D dry foams; see figure 1. Abd el Kader and Earnshaw (1998) suggested that both a finite liquid content and small statistical sample due to the finite size of a cluster were responsible for the difference between their

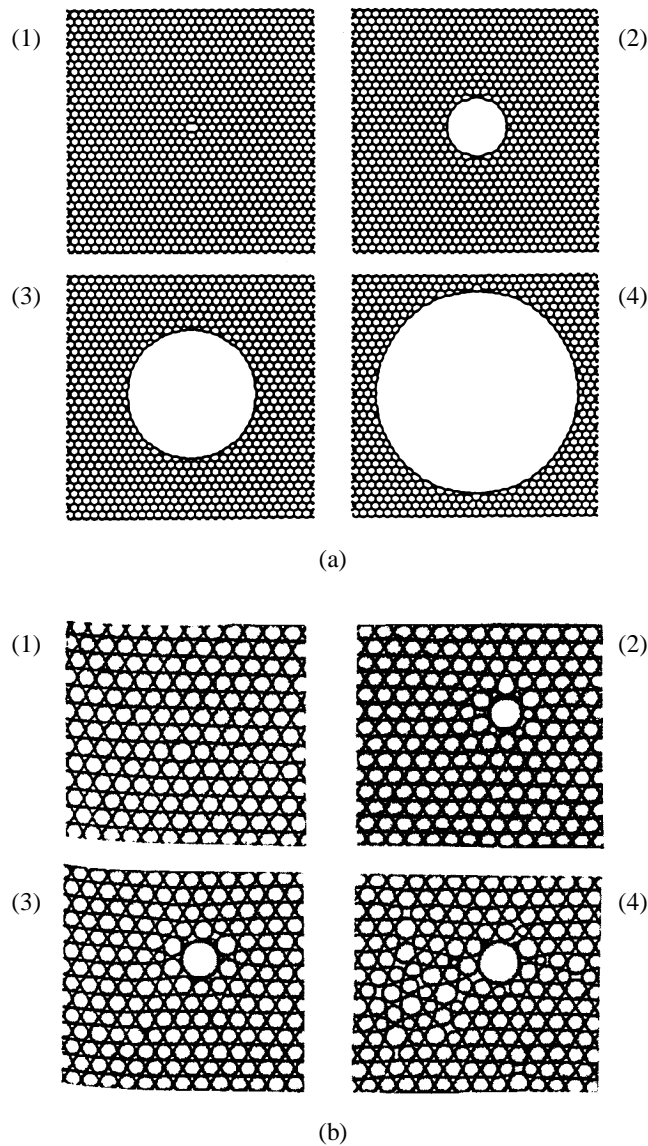


Figure 1. Snapshots of the evolution of a type 1 defect from (a) the dry-foam simulations of Chae and Tabor (1997), and (b) the wet-foam experiments of Abd el Kader and Earnshaw (1998). Dry-foam simulations predict that the number of neighbours of the defect bubble increase indefinitely, which also forces μ_2 of the cluster to increase indefinitely.

experiments and previous models.

In the last four years, a 2D bubble dynamics model was introduced by Durian (1995, 1997) to incorporate polydispersity and a finite liquid fraction into a simple simulation approach. Using a variation of Durian's 2D bubble dynamics model, in this paper we examine the evolution of two defect types, including a single large bubble of $R = 1.5\langle R \rangle_{in}$ and a cluster of bubbles of radius $R = 0.85\langle R \rangle_{in}$, inserted in a monodisperse lattice. Note that $\langle R \rangle_{in}$ denotes the average bubble radius of the initial bubble size distribution.

2. The bubble dynamics and inter-bubble gas diffusion models

The bubble dynamics model (Durian 1995, 1997) consists of a system of circular discs, with each disc interacting with surrounding discs via a repulsive force proportional to the degree of disc overlap. Bubble motion is evaluated similarly to molecular dynamics simulations (Allen and Tildesley 1992), that is, by applying Newton's second law of motion to each bubble. In addition to simplicity, there are many advantages of this bubble dynamics model over earlier models of foam, including the applicability of the model to 3D foam, the ease of accounting for a distribution of bubble sizes, and a finite liquid fraction in the simulation. Moreover, it is unnecessary to explicitly define and control the many possible bubble rearrangement processes, and various dissipation mechanisms are easily incorporated into the simulations.

Durian's model for bubble dynamics assumes that the effect of inertia on bubble motion may be neglected because of the very small mass that can be associated with bubbles. Any inertial effects are insignificant in comparison to the effects of inter-bubble compression forces and to the dissipation due to shearing in the thin film separating the bubbles. A quasi-static equation for bubble motion can be written as

$$\vec{v}_i = \frac{1}{b} \sum_{\substack{j=1 \\ j \neq i}}^N \vec{F}_{ij} \quad (1)$$

where \vec{v}_i is the velocity of the i th bubble, \vec{F}_{ij} denotes the compression force between the i th and j th bubbles. The constant b originates from shearing in thin films between bubbles and is defined by the surface area multiplied by the ratio of the liquid-phase viscosity to the thickness of the thin film. The summation is only performed over contacting or overlapping bubbles. When bubbles move according to equation (1), on average, they move in a direction which minimizes the force per bubble. If a system of bubbles is allowed to come to equilibrium by following equation (1), the excess surface energy due to bubble compression tends to a local minimum. Note that in equation (1), the effect of the relative motion of neighbouring bubbles is assumed to be insignificant in comparison to compression forces.

The interaction force between a bubble pair is modelled as being spring-like, that is, the force between contacting bubbles is proportional to the degree of overlap of the circular discs. This spring force is a function of the relative bubble positions and radii only:

$$\vec{F}_{ij} = F_0 \xi_{ij} \frac{\vec{r}_i - \vec{r}_j}{|\vec{r}_i - \vec{r}_j|} \quad (2)$$

where $F_0 \simeq \sigma \langle R \rangle$ and the non-dimensional compression of the overlapping bubble pair is

$$\xi_{ij} = \frac{R_i + R_j - |\vec{r}_i - \vec{r}_j|}{R_i + R_j}. \quad (3)$$

Initially bubbles are positioned on a 2D hexagonal lattice with lattice spacing greater than the maximum bubble diameter. Bubbles are then allocated radii as required by a simulation, and the volume of the sparse cubic lattice is decreased until the desired gas fraction is achieved. The resulting system is allowed to relax to minimize bubble overlap. This is done by determining bubble velocities from equation (1), and then using

$$\vec{r}_i(t + \Delta t) = \vec{r}_i(t) + 0.5[\vec{v}_i(t) + \vec{v}_i(t + \Delta t)]\Delta t$$

to calculate the new bubble positions. The procedure for equilibrating the system is repeated until the velocity of each bubble is zero to within numerical accuracy. A characteristic timescale for bubble rearrangements may be defined as $\tau_b = b \langle R \rangle_{in} / F_0$. The time step Δt was chosen small enough so as not to affect the behaviour of the bubble system. For our system we have

set $b\langle R \rangle_{in}/F_0 = 1$, and $\Delta t \leq 0.1$. To minimize the effects of a finite system size, periodic boundaries are used in all directions and simulations are stopped before the growing defect reaches the edge of the simulation area.

The inter-bubble gas diffusion is modelled as follows. The transfer of gas between bubbles in the model takes place between neighbouring bubbles only. The rate of transfer is assumed to be proportional to the difference in pressure between contacting bubbles, and the excess pressure (pressure above atmospheric pressure due to surface tension) in a bubble in our wet-foam model is assumed to be inversely proportional to the bubble radius. The number of moles of gas in a bubble is calculated from the ideal-gas law by noting that bubble pressure does not differ substantially from atmospheric pressure. The following expression for the transfer of gas between two contacting bubbles at each time step can then be obtained:

$$\frac{dV_{ij}}{dt} = K A_{ij} \left(\frac{1}{R_j} - \frac{1}{R_i} \right) \quad (4)$$

where

$$K = \frac{2J\sigma R_G T}{P_0}. \quad (5)$$

In equations (4) and (5), V denotes the volume of gas transferred between the two bubbles in a bubble pair, σ is the surface tension, T symbolizes temperature, P_0 is the atmospheric pressure, R_G stands for the gas constant, J is the effective permeability of gas (the overall mass-transfer coefficient) defined as the reciprocal of the sum of resistances due to mass transfer in the lamellae and the boundary layers of the two contacting bubbles, and finally A_{ij} signifies the area of the thin film between bubbles i and j . In 2D, we approximate A_{ij} by the line defined by the intersection of the two bubbles multiplied by a unit length. (Note that in 2D the simulations are actually conducted for interacting parallel cylinders.) From geometrical considerations we obtain

$$A_{ij} = 2R_i \sqrt{G(2-G)} \quad (6)$$

where

$$G = \frac{\xi_{ij}(2R_j - (R_i + R_j)\xi_{ij})}{2R_i(1 - \xi_{ij})} \quad (7)$$

and ξ_{ij} is defined in equation (3). After some cumbersome but straightforward algebra, equation (6) can be shown to be symmetric, that is $A_{ij} = A_{ji}$. The set of equations for all bubble pairs (equation (4)) conserves the gas volume of the bubble system, and therefore the gas fraction of the foam is maintained.

In the bubble dynamics model it is possible that a small number of small bubbles (<1%) may have no contacting neighbours. These bubbles are unable to exchange gas with surrounding bubbles by following equation (4). This leads to the appearance of a large number of very small bubbles which do not vanish in the course of simulations. To avoid this situation and to involve the small bubbles with no contacting neighbours in the transfer of gas, the average pressure of all bubbles in the system is determined and the gas exchange is made according to an equivalent average neighbour pressure. The expression for this process is

$$\frac{dR_i}{dt} = K \left(\left\langle \frac{1}{R_j} \right\rangle - \frac{1}{R_i} \right). \quad (8)$$

In this case the gas transfer occurs through the entire bubble surface area. Equation (8) is only applied to the small number of bubbles with no contacting neighbours. Unfortunately, equation (8) does not conserve the foam gas fraction. Therefore, a small readjustment is made to the volume of all bubbles, by an amount proportional to individual bubble radii.

A singularity in the bubble internal pressure for bubbles with $R \rightarrow 0$ is avoided by not allowing a bubble to exist if its radius is below a critical value. This occurs in real foams as well, since bubbles dissolve completely once they become very small. The minimum bubble radius is set to $0.1\langle R \rangle_{in}$. When a bubble radius falls below the cut-off threshold, the bubble disappears and the bubble gas (or area) is returned to all remaining bubbles at a fraction proportional to the individual bubble size.

The units of K are $\text{m}^2 \text{s}^{-1}$ and so in the simulations the timescale is made non-dimensional according to $t^* = Kt/\langle R \rangle_{in}^2$. To avoid bubbles being enveloped by the growth of neighbouring bubbles, K is chosen such that $\langle R \rangle_{in}^2/K$ is large in comparison to the timescale for bubble rearrangement. In the present simulations, $K = 0.0001$.

3. Defect evolution predictions

In the following section the inter-bubble gas diffusion is investigated in 2D systems consisting of monodisperse bubbles located on a lattice with a single dislocation. In all simulations, the total amount of gas contained within the system is conserved.

In referring to different defect types we adopt the classification given by Vaz and Fortes (1997). Type I defects refer to a single large bubble in an otherwise monodisperse lattice. Type II defects come in two subcategories. Type IIA refers to a defect consisting of a cluster of bubbles with radii both larger and smaller than the hexagonal lattice, but with an average bubble area smaller than that of the surrounding lattice bubbles. Type IIB clusters are identified by a cluster of bubbles exclusively smaller than the surrounding hexagonal lattice bubbles.

The following simulations are initialized with type I and type IIB defects. By investigating the evolution of type IIB defects, the development of type IIA defects is examined by default, as type IIB defects soon evolve to type IIA defects. In all cases, the bubble cluster associated with the initial defect is defined as the group of bubbles of size and arrangement different to that of the monodisperse hexagonal lattice. Note that initially the bubble systems are in equilibrium; however, bubbles do not necessarily surround the defect bubbles symmetrically. This lack of symmetry results in uneven diffusion between the initial defect cluster bubbles and eventually the general disorder observed in figure 2.

There have been several definitions of the bubble cluster in previous studies. The consistent feature of all bubble cluster definitions is their reliance on three well identifiable regions: (1) the undisturbed lattice, (2) the disturbed bubbles near the defect bubble which vary in size and in the number of neighbours from the bubbles in the surrounding lattice, and (3) the front between regions (1) and (2). On the basis of these three distinct regions, bubble clusters have been defined alternatively as the group of disturbed bubbles, the group of disturbed bubbles plus the first layer of six-sided undisturbed bubbles, and the group of bubbles within a disturbed circular front centred on the defect bubble. Each particular definition of a bubble cluster will give different values of the average number of neighbours in the cluster and the disorder. For this reason, only qualitative comparisons can be drawn among previous studies.

In the present study a bubble is included in the cluster if it satisfies either of the following criteria: $|R_i - R_0| \geq 0.1$; $0.001 \leq |R_i - R_0| \leq 0.1$ and $n_i \neq 6$ (where R_0 is the radius of a bubble in the undisturbed lattice). The second criterion is used to mimic experimental determination of the cluster. In experiments, it is very difficult to distinguish between bubble sizes; however, the number of bubble neighbours is easily determined. Hence the bubble cluster is defined by the outer circle of bubbles which have both size and number of neighbours different from the surrounding periodic lattice. Note that it is possible for a bubble to have $R_i = R_0$ or $0.001 \leq |R_i - R_0| \leq 0.1$ and $n_i = 6$ well within the cluster, and therefore be excluded from calculations. However, this occurs infrequently and has no effect on the results.

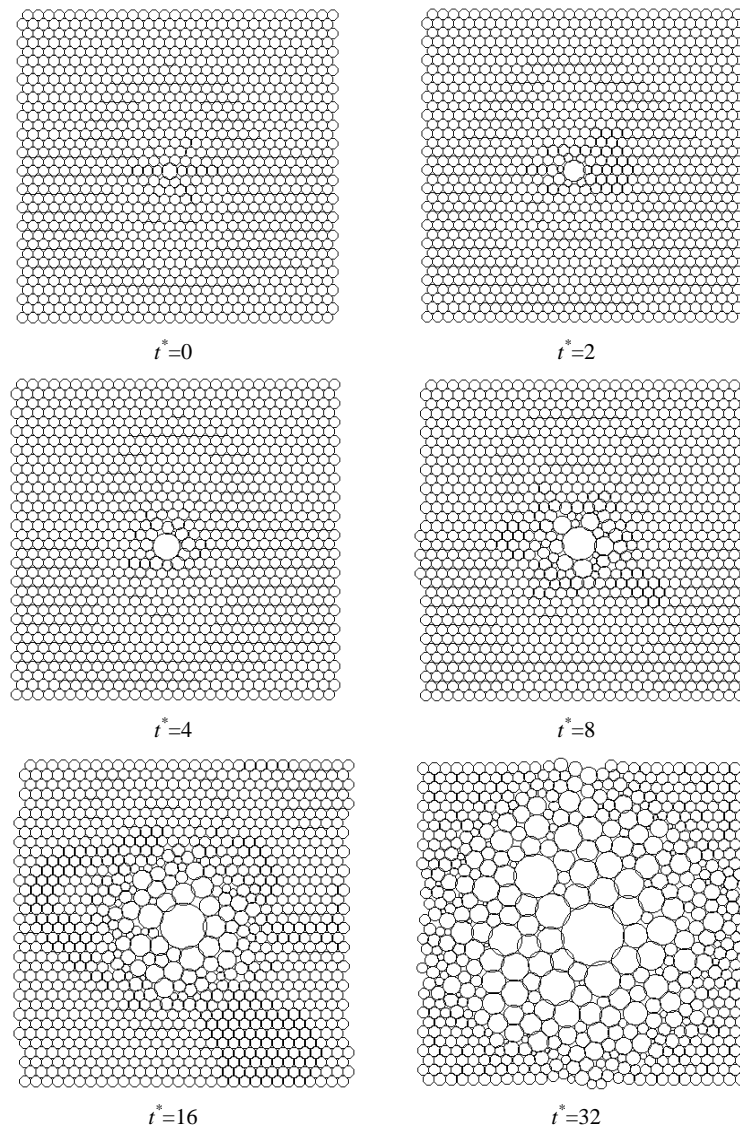


Figure 2. Snapshots in time of the evolution of a type I defect in a 2D monodisperse foam using the bubble dynamics model; $N_{in} = 1020$, $\phi = 0.95$, initial defect radius = $1.5\langle R \rangle_{in}$.

3.1. Type I defects

It is seen for the type I defect depicted in figure 2 that initially, as the defect bubble grows, the neighbouring bubbles in direct contact with the initial defect seed bubble begin to shrink. It is convenient to refer to these neighbouring bubbles as the first-shell bubbles. In the same fashion, bubbles in direct contact with the first-shell bubbles, but with no contact with the defect seed bubble, are referred to as the second-shell bubbles. As bubbles in the first shell shrink, the centre defect and bubbles in the second shell grow, on average. The oscillations in bubble size with alternate shells are restricted to the bubble cluster, and the effect soon becomes

lost as bubble motion causes inter-shell mixing. Eventually, the predominant pattern displayed is a rapid decrease in bubble sizes in a radial direction away from the centre defect bubble. The results presented in figure 2 are in qualitative agreement with the experimental findings presented in figure 1(b). Compare, for example, figure 2 ($t^* = 4$ and $t^* = 8$) with figure 1(b) (second and third snapshots). As reported in the introduction, previous numerical models of dry foams are not able to yield the coarsening behaviour observed in wet-foam experiments and in the present study on wet foams.

The increase in the number of bubbles in the cluster, the growth of the average bubble size in the cluster and the growth of the original defect bubble are shown in figures 3–5. Due to the localized inter-bubble diffusion after $t^* = 7$, large bubbles form around the centre defect bubble. As the effect of the formation of these secondary large bubbles, the number of neighbours of the original defect bubble is limited. The maximum number of neighbours for the centre defect bubble occurs at $t^* = 4$, when $n = 12$ (see figure 6). After $t^* = 7$, the number of neighbours for the centre defect bubble oscillates between 9 and 10.

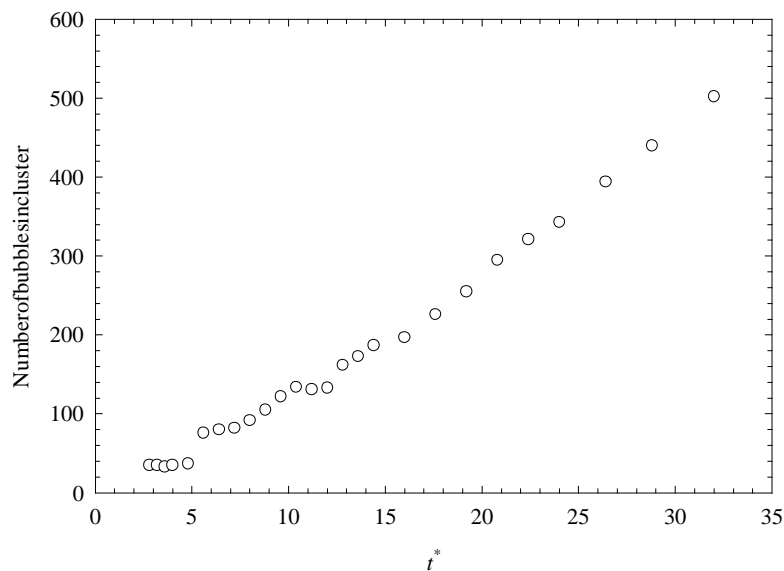


Figure 3. Growth of the number of bubbles in the cluster associated with the type I defect.

Equation (9), derived from geometrical considerations illustrated in figure 7, approximates the average number of neighbours for a bubble as a function of the defect bubble radius R_i and average radius of neighbouring bubbles $\langle R \rangle$:

$$n_i = 360^\circ / \cos^{-1} \left(1 - \frac{2\langle R \rangle^2}{(R_i + \langle R \rangle)^2} \right). \quad (9)$$

From equation (9), it is seen that the number of neighbours of a defect bubble can be related to the ratio between the size of the defect bubble and that of those surrounding it. In our simulations, the number of neighbours of the defect seed bubble and μ_2 for the cluster initially increase until relatively large bubbles appear next to the seed bubble (see figures 6 and 8); μ_2 denotes the second moment of the distribution of the number of contacting neighbours. This behaviour has also been observed in the 2D wet-foam experiments of Abd el Kader and Earnshaw (1998). Equation (9) predicts $n = 10$ for the defect bubble, with $\langle R \rangle = 2$ and $R = 4.5$, which corresponds approximately to conditions at $t^* = 20$ (see figure 5). Note that

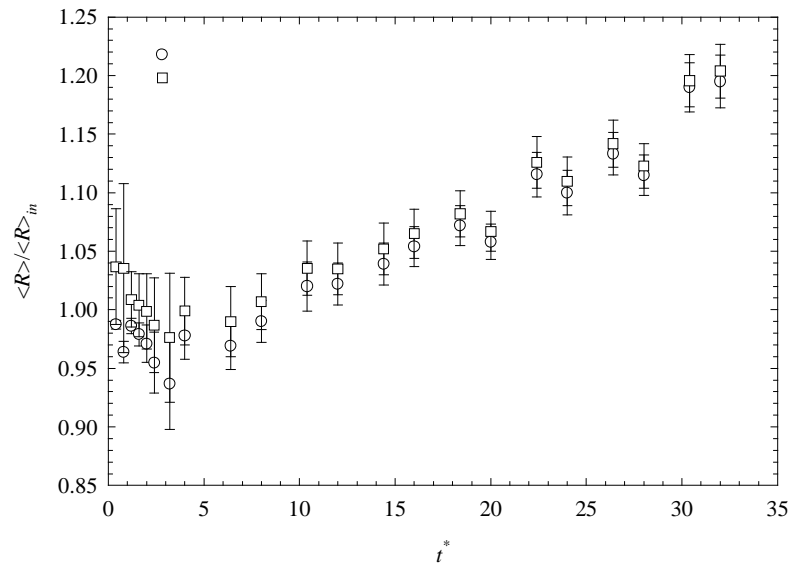


Figure 4. Growth of the average bubble size in the cluster associated with a type I defect, including and excluding the initial defect bubble.

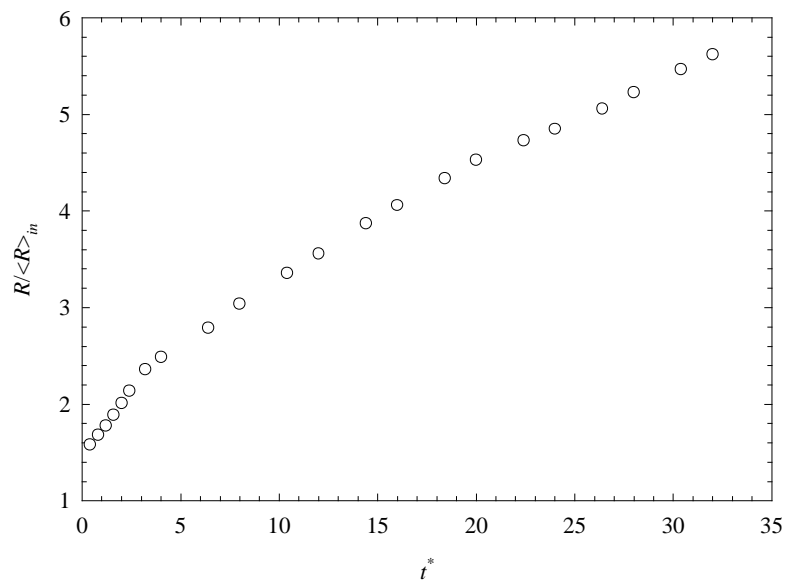


Figure 5. Growth in radius of the type I defect seed bubble.

if an average diffusion equation, such as equation (8), was used irrespective of the number of neighbours, only two bubble sizes would be present. In this case, the number of neighbours of the defect bubble and μ_2 would grow indefinitely.

In their simulations of the evolution of a single bubble defect (see figure 1), Chae and Tabor (1997) used a two-step model. In the first step, mass transfer from or to a given bubble was calculated from von Neumann's cell growth law. This was followed by a relaxation step,

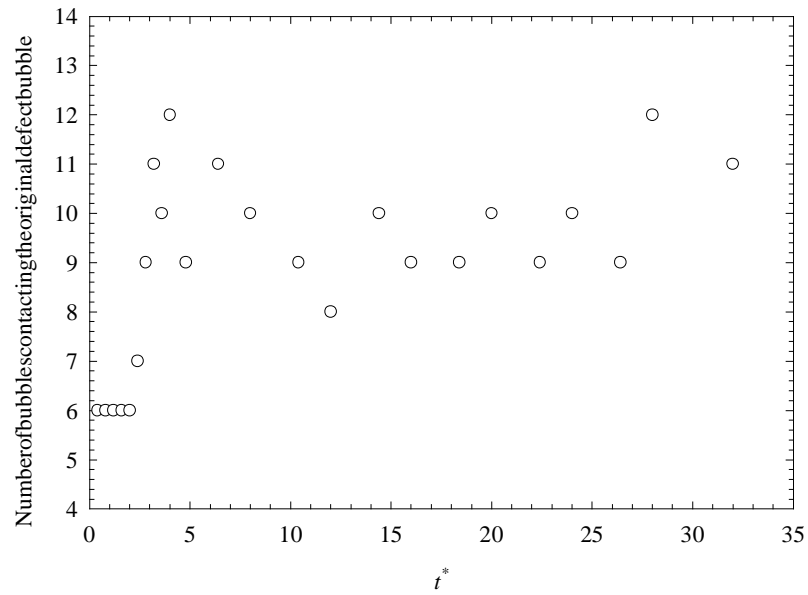


Figure 6. The change in the number of contacting bubbles for the original defect bubble in the type I defect.

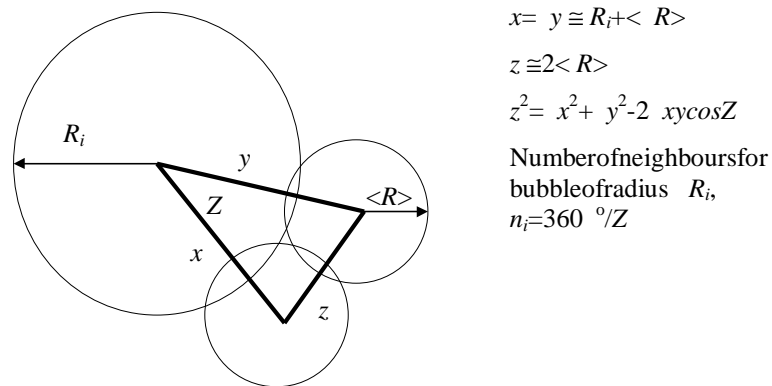


Figure 7. A diagram illustrating how the difference between the size of the central bubble and that of the surrounding bubbles determines the number of contacting neighbours of the central bubble.

which included adjustments to lamellae (called edges in 2D geometry) and vertex movement. The number of neighbours of a bubble generally changes during foam evolution. This was handled in their model by T2 transformations (disappearance of a bubble) in the cell growth stage and T1 transformations (the neighbours change, which occurs when two bubbles come together by pushing the other two bubbles apart) in the vertex movement stage. There was a degree of arbitrariness in the model related to the implementation of T2 transformations of four- and five-sided bubbles (called cells in 2D geometry), leading to different foam evolution trajectories. However, the major difference between Chae and Tabor's work and the present

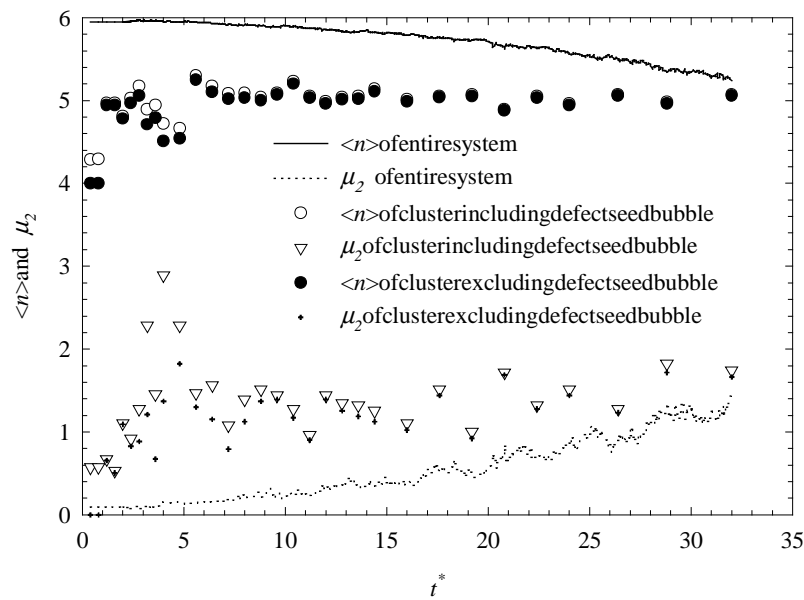


Figure 8. Evolution of a type I defect—in particular, the evolution of the average number of neighbours per bubble and μ_2 for the bubble cluster, including and excluding the original defect bubble, and the entire bubble system; $N_{in} = 1020$, $\phi = 0.95$, initial defect radius = $1.5\langle R \rangle_{in}$.

paper lies in the inclusion of liquid fraction in our model, resulting in a physically realistic prediction of defect cluster evolution.

However, von Neumann's law is only valid locally, that is for each cell separately, for perfectly dry foam in which internal angles of cells are exactly 120° . With an increasing liquid fraction, the law loses its strictly local validity (Glazier and Weaire 1992) and then it ceases to apply even on average. For liquid fractions considered in this work, the law is not valid at all. In polydisperse, wet foams, bubble evolution is a result of direct gas diffusion between neighbouring bubbles through thin films, with the internal angles of cells being away from their equilibrium values of 120° . More importantly in wet foams, the vertex movement together with T1 and T2 transformations arise as a result of bubble motion in the liquid matrix and there is nothing arbitrary about it. The motion of bubbles and their growth are governed by the deterministic bubble evolution equations.

It is interesting to compare our results, suggesting that the number of neighbours of the defect seed bubble is limited by the decrease in the ratio between the average neighbour bubble size and the defect seed bubble size (figures 2 and 6), with those of Stavans and Glazier (1989). Stavans and Glazier commented that variations of vertex angles away from 120° result in large strain energies in the film structure, making the occurrence of many-sided bubbles unlikely. To demonstrate this, they produced a large 20-sided bubble which displayed vertex angles distinct from 120° . Typically, a bubble of this type was observed to evolve to having 11 or 12 sides, which incidentally compares well with results from our simulations, in which the number of neighbours of the large defect seed bubble is between 9 and 12 (figure 6).

Images provided by Stavans and Glazier (1989), of the evolution of a large many-sided bubble, clearly show that initially the bubble is surrounded by much smaller bubbles. However, at the end of the evolution process, the size of the neighbouring bubbles relative to the large bubble had decreased, along with the number of sides. This is consistent with the predictions

of equation (9) for spherical bubbles. Also it can be shown (figure 7) that the greater the ratio between bubble sizes in our simulation, the larger the vertex angle:

$$V_{angle} = 180^\circ - \cos^{-1}\left(1 - \frac{2\langle R \rangle^2}{(R_i + \langle R \rangle)^2}\right). \quad (10)$$

The average vertex angle predicted for the defect bubble, with $\langle R \rangle = 2$ and $R = 4.5$, is 144° .

It is seen in figure 8 that, below $t^* = 4$, the second moments μ_2 for the entire system and for the bubble cluster, including and excluding the seed defect bubble, increase as the foam evolves. After an initial rise, the value of μ_2 , for a cluster which excludes the seed bubble, attains a value of 1.3 ± 0.2 which is then maintained (or increases slightly) throughout the simulation. The average number of neighbours per bubble for the cluster, including and excluding the seed defect bubble, reaches a constant value of $\langle n \rangle = 5.0$ to 5.1 . These results agree with experiments (Vaz and Fortes 1997, Abd el Kader and Earnshaw 1997, 1998) and the simulations of Ruskin and Feng (1995) and Jiang *et al* (1995).

At $t^* = 4$, μ_2 for the cluster which includes the defect seed bubble reaches a maximum of 2.9 before returning, at $t^* = 6$, to a level similar to that for a cluster which excludes the seed bubble ($\mu_2 = 1.3 \pm 0.2$). After $t^* = 6$, μ_2 rises for the entire bubble system. However, for the cluster including the defect bubble, a transient state occurs in which the cluster's disorder is relatively stable (or increasing slowly) at a level lower than that of a polydisperse model foam in a scaling state (Gardiner *et al* (1999); $\mu_2 = 2.1 \pm 0.1$). At long timescales (not shown), μ_2 for the cluster increases to match that of a polydisperse model foam in the scaling state, as the cluster begins to resemble a polydisperse foam. The observation of a transient state is in contrast to previous simulations, but it is however in agreement with recent experiments (Abd el Kader and Earnshaw 1998). Experiments conducted at timescales similar to those used in simulations are clearly required.

The majority of simulation studies including the present investigation find that μ_2 initially increases monotonically. A similar behaviour is observed in short-lifetime experiments in which the change in area of the defect bubble has less than doubled (Vaz and Fortes 1997, Abd el Kader and Earnshaw 1997). A major difference occurs between long-time behaviour of the defect cluster predicted by the present model and the results of the majority of previous simulations. Previous simulations, excluding those of Levitan (1994), predict that μ_2 for the entire bubble cluster increases indefinitely, with the number of neighbours of the defect bubble also growing continuously. Recent long-timescale experiments on 2D wet foams (Abd el Kader and Earnshaw 1998) reveal that the number of neighbours of the defect bubble is limited, as is μ_2 , in agreement with our simulations. The agreement between the long-time behaviour of our simulations and recent experiments may be due to the presence of a finite liquid fraction in this study which, unlike previous simulations, is concerned with wet foams.

3.2. Type II defects

Type IIA and IIB defects have been investigated in the experiments of Vaz and Fortes (1997). Vaz and Fortes found that type IIB defects soon evolve into type IIA defects. This occurs because some of the small bubbles in the cluster liberate their gas to the nearby lattice bubbles and disappear to leave a cluster of large bubbles. As illustrated in figure 9, the present simulations reproduce the transition from type IIB to type IIA defects quite well.

The general long-time trend in the evolution of type IIA and IIB defects, as with type I defects, displays a radial decrease in bubble size, centred about the initial defect seed cluster. The number of bubbles and the average size of a cluster bubble generally increase with time, as demonstrated in figures 10 and 11. A rapid initial increase in the average bubble size in

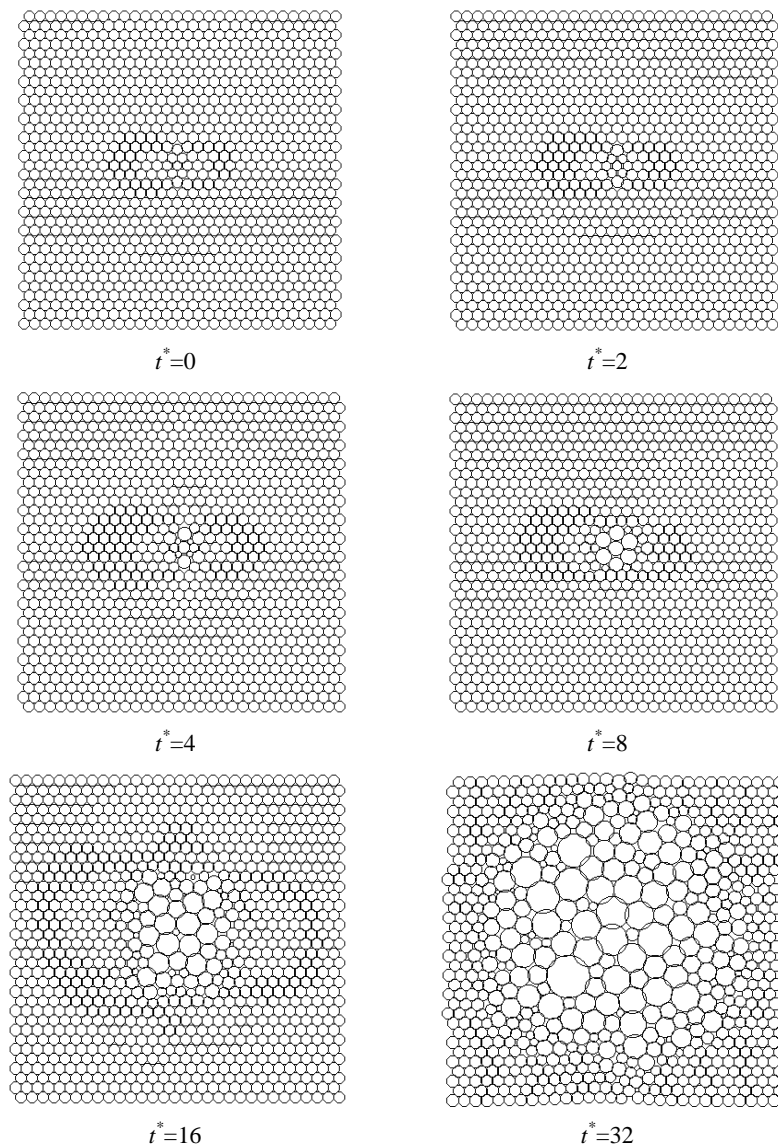


Figure 9. Snapshots in time of the evolution of a type IIB defect in a 2D monodisperse foam; $N_{in} = 1020$, $\phi = 0.95$, initial defect cluster bubble radii $= 0.85\langle R \rangle_{in}$.

figure 11 represents the disappearance of the small cluster bubbles, liberating their gas to form large bubbles.

Agreement between our simulations and the short-timescale experiments of Vaz and Fortes (1997) is found with the size of the bubble cluster initially contracting before increasing. At longer timescales we find μ_2 reaching a constant level within a transient state, with $\mu_2 = 1.3 \pm 0.3$ (figure 12). This result is surprisingly similar to the case of a type I defect. Again the transient value of μ_2 is less than that found in the scaling regime of polydisperse foam of $\mu_2 = 2.1 \pm 0.1$. An explanation of this transient scaling regime in our defect clusters is yet to surface.

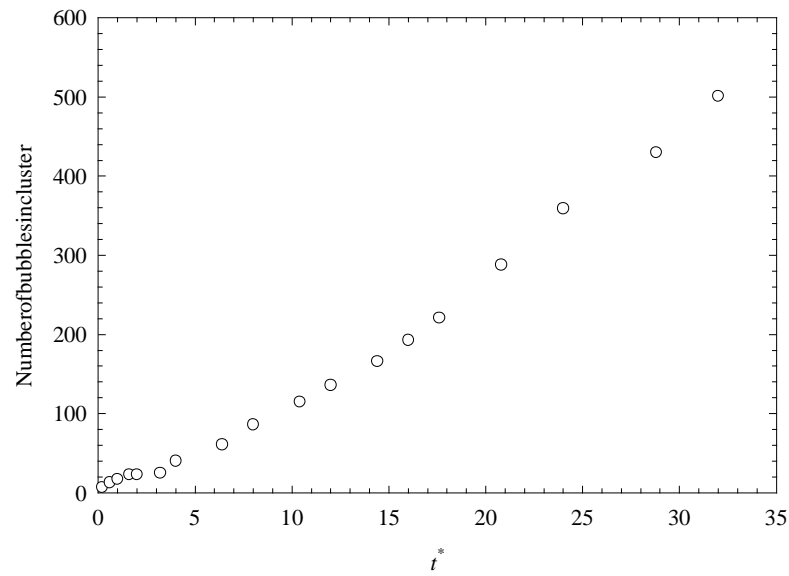


Figure 10. Growth of the number of bubbles in the cluster associated with the type IIB defect.

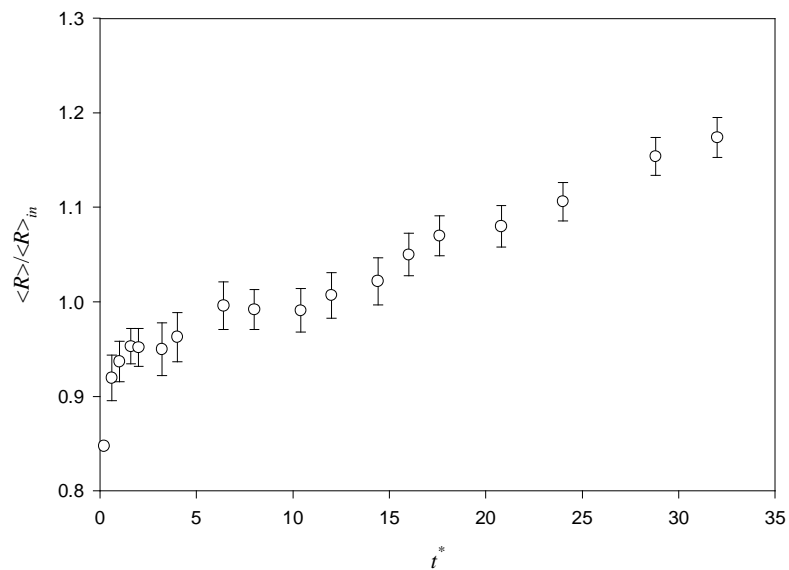


Figure 11. Growth of the average bubble size in the cluster associated with a type IIB defect.

4. Conclusions

By basing the simulation on the bubble dynamics model we have been able to simulate 2D wet foam undergoing coarsening. In particular, we have shown the evolution of defects in otherwise monodisperse perfect bubble lattice. The bubble dynamics model governs the movement of bubbles and hence it circumvents the need for the many types of bubble rearrangement events to be considered explicitly. As the bubble dynamics model allows a finite liquid content to be

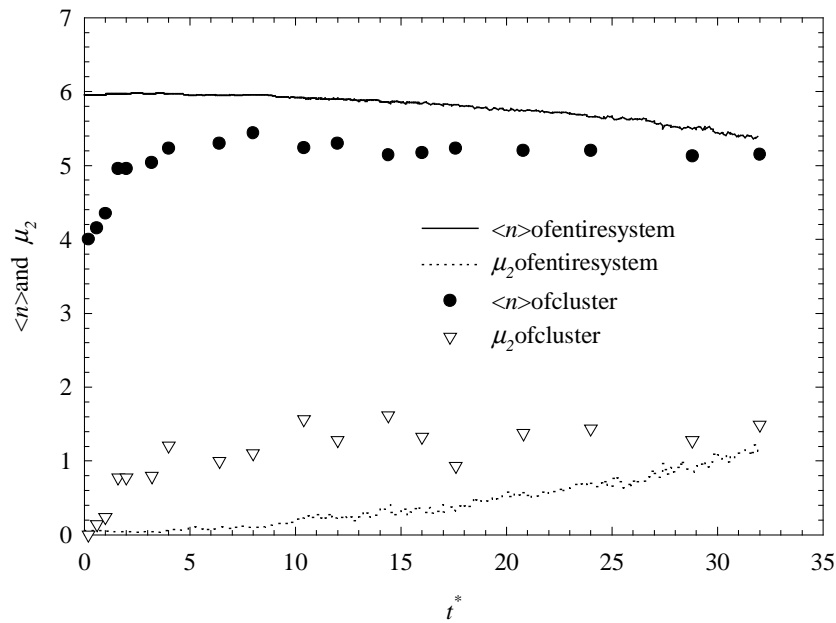


Figure 12. Evolution of a type IIB defect—in particular, the evolution of the average number of neighbours per bubble and μ_2 for the bubble and the entire bubble system; $N_{in} = 1020$, $\phi = 0.95$, initial defect bubble radii $= 0.85\langle R \rangle_{in}$.

included in simulations, unlike previous dry-foam diffusion models, direct comparisons can be made with the results from recent 2D wet-foam experiments.

The present model predicts that the disorder around a defect initially grows, before reaching a regime characterized by a relatively constant value of the average number of neighbours and μ_2 . In the transition between growth of disorder and relatively stable disorder, the disorder of the cluster associated with the point defect may increase or decrease to levels different from that of a foam in a scaling regime. These findings are generally consistent with long-timescale experiments of Abd el Kader and Earnshaw (1998) but differ from predictions of previous simulations performed on dry foams. Our result supports the hypothesis of Abd el Kader and Earnshaw (1998) that differences between experiments and previous simulations may be due to the liquid content of real foams.

In the wet-foam simulations and experiments, entire bubbles move to minimize compression or excess surface energy. The vertex movements, as well as T1 and T2 transformations occur naturally, without arbitrariness, as a result of bubble motion. This is especially important for a large growing bubble, which engenders movement of the surrounding bubbles. Finally, we have indicated that von Neumann's law is strictly valid for perfectly dry foams, which are very difficult (if not impossible) to reproduce in experiments of single-defect evolution. Consequently, the modelling of this evolution process must account for the liquid fraction, as is done in the present study.

Acknowledgments

The authors wish to acknowledge helpful discussions with Dr A Abd el Kader of the Queen's University of Belfast. This study was funded by the Australian Research Council.

Appendix. Nomenclature

In the following list of nomenclature, (—) indicates non-dimensional variables.

A	surface area (m ²)
b	shearing constant used in equation (1) (kg s ⁻¹)
D	bubble cluster diameter (m)
\vec{F}_{ij}	force due to compression between the i th and j th bubbles (N)
F_0	spring force constant (N)
G	constant defined by equation (7) and used in equation (6) (—)
J	permeability coefficient (mol N ⁻¹ s ⁻¹)
K	permeability constant (m ² s ⁻¹)
N	number of bubbles in the simulation (—)
n	number of bubbles contacting the i th bubble (—)
$\langle n \rangle$	average number of contacting neighbours per bubble (—)
P_0	pressure in Plateau borders (Pa)
R	bubble radius (m)
\vec{r}	bubble position (m)
$\langle R \rangle$	average bubble radius (m)
R_G	gas constant (N m mol ⁻¹ K ⁻¹)
R_0	radius of an undisturbed lattice bubble (m)
$\langle 1/R_j \rangle$	the equivalent average bubble radius to give the average internal bubble pressure (m ⁻¹)
T	temperature (K)
t	time (s)
t^*	non-dimensional time (—)
V	volume (m ³)
V_{angle}	vertex angle of a Plateau border (degrees)
\vec{v}	bubble velocity (m s ⁻¹)
ϕ	gas fraction (—)
μ_2	second moment of the distribution of the number of contacting neighbours per bubble (—)
σ	surface tension (N m ⁻¹)
τ_b	bubble rearrangement timescale (s)
ξ	non-dimensional compression (—)

Subscripts

i, j	refer to bubbles i and j respectively
ij	refers to the interaction between bubbles i and j
in	refers to the initial value of a variable, i.e. that at $t = 0$

References

- Abd el Kader A and Earnshaw J C 1997 *Phys. Rev. E* **56** 3251
 Abd el Kader A and Earnshaw J C 1998 *Phys. Rev. E* **58** 760
 Aboav D A 1980 *Metallography* **13** 43
 Allen M P and Tildesley D J 1992 *Computer Simulation of Liquids* (New York: Oxford University Press)

- Chae J J and Tabor M 1997 *Phys. Rev. E* **55** 598
Durian D 1995 *Phys. Rev. Lett.* **75** 4780
Durian D 1997 *Phys. Rev. E* **55** 1739
Vaz M F and Fortes M A 1997 *J. Phys.: Condens. Matter* **9** 8921
Gardiner B S, Dlugogorski B Z and Jameson G J 1999 *Phil. Mag. A* at press
Glazier J A and Weaire D 1992 *J. Phys.: Condens. Matter* **4** 1867
Herdtle T 1991 *PhD Dissertation* University of California, San Diego, CA
Jiang Y, Mombach J C M and Glazier J A 1995 *Phys. Rev. E* **52** R3333
Levitan B 1994 *Phys. Rev. Lett.* **72** 4057
Ruskin H J and Feng Y 1995 *J. Phys.: Condens. Matter* **7** L553
Stavans J and Glazier J A 1989 *Phys. Rev. Lett.* **62** 1318
Weaire D 1995 *Phys. Rev. Lett.* **74** 3710
Weaire D and Lei H 1990 *Phil. Mag. Lett.* **62** 427